Journal of Thermal Analysis and Calorimetry, Vol. 61 (2000) 551–564

SYMMETRIC BLOCK OLIGOMERS
Gelation characteristics by DSC

E. G. Fernandes[1], *S. Krauser*[2], *C. M. Samour*[2] *and E. Chiellini*[1*]

[1]Department of Chemistry and Industrial Chemistry, Pisa University, via Risorgimento 35 56126 Pisa, Italy
[2]MacroChem Corporation, 110 Hartwell Avenue, Lexington MA 02421, USA

Abstract

Symmetrical block oligomers having in common terminal groups (A) consisting of polyoxyethylene (20) stearyl ether are materials of pharmaceutical and cosmetic interest. Phase properties of their aqueous systems and amounts of water typologies were determined by differential scanning calorimetry (DSC).

The overall amount of water absorbed by each investigated oligomer was not significantly influenced by the type of central bridging block, whereas the amount of free water decreased with increasing oligomer concentration in the gel. A number of 60–70 moles of water was found to solvate the oligomer chain. The oligomers studied presented a thermo-reversible gelation with and precipitation under determined temperature conditions.

Keywords: amphiphile oligomers, DSC, thermo-reversible gelation, water states

Introduction

For topical preparations, the permeability of an active substance depends not only on its properties but also on the nature of the formulation [1]. Permeability may increase with an increase in the water content of the stratum corneum (SC- the least permeable skin stratum), surface tension reduction or by membrane expansion [2]. The diffusion of a molecule across a membrane depends on the cooperative motions of units of the macromolecules that compose the membrane. The mobility of a macromolecule is related to properties such as glass transition temperature, crystallinity and interactions between components of the system [3].

The symmetric amphiphilic urethane block oligomers presented in this work consist of two terminal segments (A) of a non-ionic surfactant and a central segment with specific functions (Scheme 1). From the blocks within polyoxyethylene (20) stearyl ether, it is expected that these will be promotion of interactions with lipid layer of skin in a similar way to that observed with non-ionic surfactants [4]. An understanding of their interactions with water is valuable not only for pharmaceutical

* Author for correspondence: Fax:+39 050 28438, E-mail: chlmeo@dcci.unipi.it.

1418–2874/2000/ $ 5.00
Akadémiai Kiadó, Budapest

formulators of controlled release systems but also for the general physico-chemical aspects that may provide insights for other fields of application. The symmetric block oligomers-water system can be considered to form associations observed on triblock copolymers end capped with hydrophobic blocks [5]. These associations are induced by temperature, forming phases that can vary from micelles to gels according to concentration.

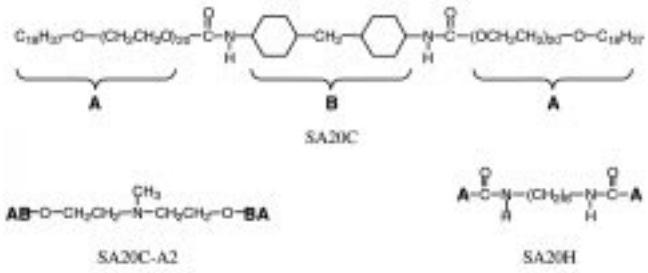

Scheme 1 Structure of the amphiphilic urethane oligomers

In the present work, phase characteristics and states of associated water have been investigated by DSC of three aqueous systems containing symmetric amphiphilic urethane block oligomers.

Experimental and materials

Analytical Methods

Thermal characteristics of oligomer/water systems were obtained from measurements using a Mettler TA4000 System instrument. It consists of a DSC-30 cell, a TG50 furnace with an M3 microbalance, and TA72 GraphWare software.

DSC analyses were performed under nitrogen flow (ca 80 ml min^{-1}). Samples of about 10 mg were weighed in a hermetic aluminium pan (40 µl capacity). The reference used was an inert material (aluminium) with a mass comparable to that of the sample.

In the method used, the high enthalpy of water in relation to that of oligomers resulted in two effects: 1) On cooling, high water content increased the sample temperature, resulting in DSC traces inclined towards the high temperature side. The upper limit of water mass complying with a DSC within the scale was ca. 4 mg; 2) On heating, the amplitude of the water melting peak increased with increasing content, thus obscuring the block oligomer transition.

Consequently, for each sample property a specific temperature range was defined. All methods began with cooling followed by heating, both at 10°C min^{-1}. To characterize the gel phase, samples were scanned from 60 to –15°C (limit reached without water crystallization). In the case of second order transition of oligomers in the gel form, the temperature range scanned was from –20 to –100°C. Finally, to analyze the water phases, samples were scanned from 60 to –100°C.

Thermogravimetric analysis was used for the evaluation of total water content. The samples were heated at 10°C min^{-1} from 25 to 500°C under nitrogen atmosphere (ca 200 ml min^{-1}). In general, about 20 mg of sample mass was used. The measurements were carried out in 70 μl alumina crucibles covered with a perforated lid.

Gel preparation

Table 1 shows characteristic properties of symmetric block oligomers used in gel preparations. Brij 78, a stearyl ether of PEG20 was used as reference.

Table 1 Thermodynamic parameters for the amphiphilic oligomers as investigated by thermal analysis

Sample	*MW*	Brij[a]	T_{g1}/	T_{g2}/	T_{c1}/	ΔH_{c1}/ J g^{-1}	T_{c2}/ °C	ΔH_{c2}/ J g^{-1}	T_{rc3}/ °C	ΔH_{rc3}/ J g^{-1}	T_m/ °C	ΔH_m/ J g^{-1}
				°C								
Brij 78	1152	1.00	–	–39.0	–	–	15.2	165.3	–	–	41.3	165.8
SA20H	2468	0.93	–49.1	–28.4	2.5	32.6	18.5	56.0	1.7	15.2	38.6	112.7
SA20C	2562	0.90	–48.0	–25.1	0.5	36.3	16.7	45.1	3.7	17.9	36.9	104.0
SA20C-A2	2943	0.78	–44.9	nd	–13.2	10.1	16.3	37.6	2.2	22.1	34.3	95.3

[a]Mass fraction of the Brij 78 segment in the oligomer sample

SA20C/water systems were prepared at nine concentrations between 0.05–0.7 w/w of oligomer, whereas, both SA20C-A2/water and SA20H/water systems were prepared at three concentrations: 0.2, 0.4, 0.6 w/w of relevant oligomer.

In a covered glass bottle, oligomer and water were mixed using an ultrasonic bath (working frequency ca 47 kHz) for 2 h at ca 50°C. At the end of mixing, the samples were allowed to cool in the bath without sonication.

Transition temperatures were not reproducible for freshly prepared sample preparations. Reproducibility was obtained when measurements were carried out two weeks following sample preparation, with storage at ambient conditions.

Results and discussion

Oligomers characterization

Figure 1 shows typical DSC traces recorded under cooling and heating of the symmetric block oligomers and Brij 78. All samples demonstrated multiple exotherms on cooling. In the case of oligomers, the higher temperature exotherm had a shoulder like that of Brij 78. Besides, their maximum peak temperatures (T_{c2}) indicated that it was affected by the bridging group connecting the two lateral polyoxyethylene stearyl ether segments A. In SA20H oligomer which consists of a hexamethylenediurethane segment as bridging group, the T_{c2} was 18.9°C, whereas, in both SA20C and SA20C-A2 oligomers, whose bridging groups contain either one or two 4,4'-urethanecyclohexylmethane moieties, a value of 16.3°C was recorded for T_{c2} . Maximum

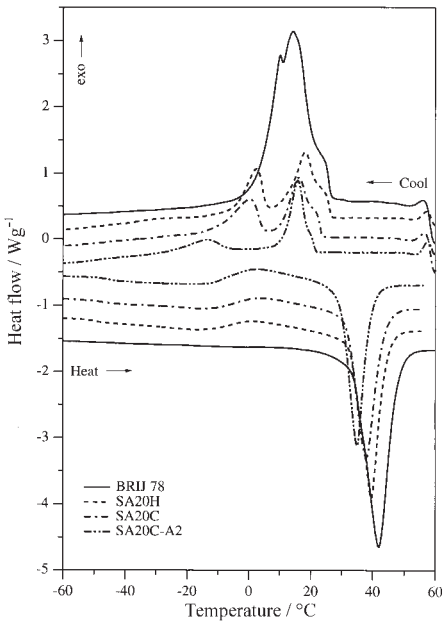

Fig. 1 DSC traces of symmetric block oligomers under cooling and heating modes

peak temperature (T_{c1}) of the lower temperature exotherm decreased as mass fraction of Brij 78 on the oligomer molecule decreased. This transition in Brij 78 was almost completely overlapped with the higher one.

On heating, a small and broad exotherm appeared preceeding the melting transition. This transition was observed at both 2°C min^{-1} and 10°C min^{-1} scan rates. The detection of an exotherm on heating may be the result of a non-complete homogeneity of the samples or may be an additional solid-solid or mesophase transition [6]. It is most likely that this exothermic peak is related to the presence of a sort condis crystal (conformationally disordered crystal). Wunderlich and Chen [7] stated that a condis crystal is a mesophase more closely related to the crystalline state with translational and orientational long-range order, but with some or full 'conformational disorder'. These characteristics are present in macromolecules that alternate segments of different chemical nature along the chain such as the samples under investigation. The maximum peak temperature (T_{rc3}) of this transition was between 2 and 3°C.

The melting enthalpies (ΔH_m) and temperatures (T_m) showed a direct relationship with the mass fraction of Brij 78 in each symmetric block oligomer.

Two glass transition temperatures were detected in two oligomers (SA20C and SA20H) whereas the lower glass transition temperature (T_{g1}) was not detected on Brij 78 and the higher glass transition temperature (T_{g2}) corresponding to that presented by Brij 78 was not detected in oligomer SA20C-A2. T_{g1}'s ranged from –45 to –49°C whereas T_{g2} ranged from –39 (Brij 78) to –25°C. The presence of two distinct glass transitions in oligomers SA20C and SA20H suggests microphase separation.

Characterization of oligomer-water systems

The term gel used in this work is not exactly that proposed by Ferry [8] but rather that describing a pharmaceutical semisolid [9]. Accordingly, 'gels are semisolid systems of either suspensions made up of small inorganic particles or large organic molecules interpenetrated by a liquid. Single-phase gels consist of organic macromolecules uniformly distributed throughout a liquid in such a manner that no apparent boundaries exist between the dispersed macromolecule and the liquid'.

The SA20C/water system showed two phases for compositions up to 0.2% w/w of SA20C: dispersion and soft mobile gel. The majority of the liquid phase was transferred to another tube following two months storage from gel preparation prior to its characterization. The SA20C/water system at higher concentration were immobile and indicated as 'hard gels'. Above 0.5% w/w of SA20C the translucid gels became opaque. The final sample compositions estimated by thermogravimetry are indicated in Table 2. Results showed that about 0.2% w/w of SA20C was the minimum mass content required to form a gel phase.

Table 2 Oligomer concentrations in oligomer/water systems[a]

SA20C		SA20C-A2		SA20H	
Nominal/ w/w	Found/ w/w	Nominal/ w/w	Found/ w/w	Nominal/ w/w	Found/ w/w
0.05	0.19				
0.10	0.21				
0.20	0.22	0.20	0.31	0.20	0.25
0.30	0.30				
0.40	0.40	0.38	0.30[b]	0.39	0.39
0.50	0.50				
0.58	0.59	0.57	0.57[b]	0.58	0.58
0.68	0.69				

[a]Nominal concentration on the basis of formulation condition and Found concentration on the basis of thermogravimetry
[b]Mean values

SA20C-A2/water systems were more opaque than that of SA20C. On the other hand, SA20H/water system were clearer and more homogeneous than that of the others oligomers. Both systems were hard gels for the higher concentrations and only the concentration of 0.2 w/w presented two phases as observed for SA20C.

DSC scans covering the temperature range from 60 to –120°C at 10°C min^{-1}, demonstrated three transitions: i) First order transition for symmetric block oligomer (a); ii) First order transition for water (b); and, iii) Two second order transitions for symmetric block oligomer (c), as exemplified by sample 0.5 w/w SA20C/water system in Fig. 2. The resolution of these transitions depended on the oligomer/water composition. In the case of SA20C/water system, that covered a larger composition

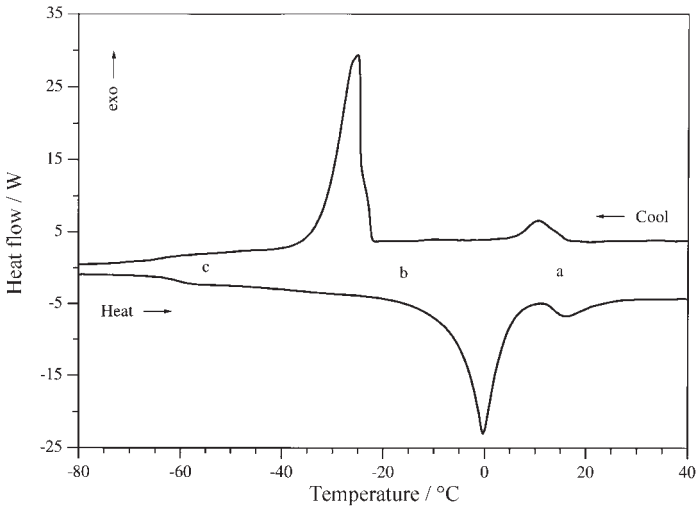

Fig. 2 DSC traces for 0.5 w/w SA20C/water system under cooling and heating modes. Scan rate=10°C min^{-1}. a) first order transition for oligomer; b) first order transition for water; c) second order transitions for oligomer

range, it was observed that, on heating, all transitions were well defined for concentrations of 0.6 and 0.7 w/w of SA20C. However, at 0.5 and 0.4 w/w concentrations, the first order transition of water overlapped that of SA20C. At lower concentrations, no further indication of the presence of SA20C first order transition was obtained. On the other hand, both SA20C and water first order transitions were well separated on cooling for all concentrations. These observations are also valid for the other oligomers-water systems. Consequently, the method to detect each thermodynamic property was amended as mentioned previously.

Glass transition determination

The SA20C/water system showed two glass transition temperatures as was observed for pure oligomer. In general, the higher glass transition temperature (T_{g2}), overlapped the beginning of the water melting. As a consequence, the T_gs were obtained from the inflection point of the heat capacity change because it is independent of transition limits.

Figure 3 and Table 3 show the dependence of SA20C/water glass transition temperatures on composition. All T_gs showed a positive deviation from additive traces (for water a T_g of –135°C was assumed [10]). Between 0.3–0.6% w/w, both T_gs were approximately constant and parallel. The mean value of T_{g2} was –39.1, 15.3°C lower than that for pure SA20C (–23.8°C); for T_{g1} the average value was –60.7 being 13.3°C lower than that for pure SA20C (–47.4°C).

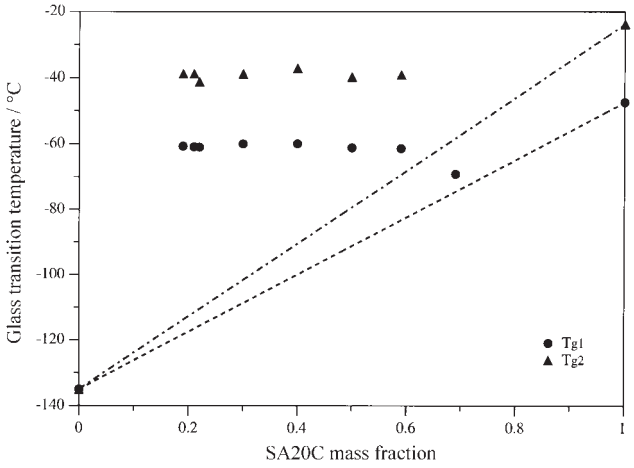

Fig. 3 Glass transition temperatures (T_{g1} and T_{g2}) as a function of SA20C-water system composition

Table 3 Glass transition temperatures in oligomer/water systems as a function of composition

SA20C			SA20C-A2			SA20H		
Conc./ w/w	T_{g1}/°C	T_{g2}/°C	Conc./ w/w	T_{g1}/°C	T_{g2}/°C	Conc./ w/w	T_{g1}/°C	T_{g2}/°C
0.19	–60.7	–38.8						
0.21	–60.9	–38.8						
0.22	–61.0	–41.2	0.31	–59.2	nd	0.25	–60.9	–38.5
0.30	–60.0	–38.8						
0.40	–59.9	–37.1	0.30	–59.9	nd	0.39	–60.8	–38.1
0.50	–61.1	–39.7						
0.59	–61.4	–39.1	0.57	–60.4	nd	0.58	–61.4	–38.1
0.69	–69.2	nd						
1.00	–48.0	–25.1	1.00	–44.9	nd	1.00	–49.1	–28.4

The glass transition temperature of pure SA20C did not correspond to 100% of amorphous phase. This meant, it was not possible to freeze the melt phase with the instrumental quenching of 100°C min^{-1}. Thus, the T_g of analyzed SA20C sample was higher than that of 100% amorphous phase due to the presence of the crystalline phase acting as a physical cross-link. On the other hand, the T_gs of SA20C/water system had at least two concurrent factors that may be responsible for their values: the crystal water that could retard the mobility of the amorphous phase (increase T_g) and water interaction with the hydrophilic groups of SA20C adding a plasticizer effect (decrease T_g).

The 0.69 w/w SA20C composition did not show water crystallization on cooling. On heating, only T_{g1} was observed because water re-crystallization occurred in

the same temperature range of T_{g2}. Nevertheless, this T_{g1} value was lower than those for the others compositions (ca 8.5°C). This can be attributed to a plasticizing effect of water, considering that the water crystals were not present. Moreover, the value of T_{g1} is close to the theoretical value.

For this type of system, the invariability of glass transition temperature with oligomer concentration may be explained as an effect that combines liquid-liquid (L-L) phase separation with vitrification. This effect is claimed to be one of the possible driving forces for gel formation [11, 12]. In general, T_g decreases by addition of solvent. In systems that show a L-L phase separation in the phase diagram, if the T_g-concentration curve intersects this line, a point called Berghmans point (BP) may be determined. At this point, the segregated phase of high solute concentration will vitrify. Consequently, if the solution concentration is within the biphasic region of L-L line, the phase separation will cease and its phase morphology will be frozen resulting in a T_g invariance. When this phase morphology presents connectivity between solute entities gelation occurs.

For the SA20C-A2/water system, only one T_g was detected on both cooling and heating scans. This transition corresponded to the lower transition temperature of SA20C/water system (Table 3). In the composition range of 0.3–0.6 mass fraction of SA20C-A2, the invariability of T_g with concentration was also observed. So, the same considerations as for SA20C hold for this case and the mean value of T_g should be in the BP zone.

The mean value for T_{g1} was –59.8°C with a decrease of 14.9°C from pure oligomer which was slightly higher than that of SA20C.

The SA20H/water system followed the same behavior as the other oligomers as can be noted from data given in Table 3. However, in this case, it was possible to detect the higher T_g on cooling. The invariable T_gs, observed in the same range of composition as the other systems, have mean values similar to those previously found: T_{g1} equal to –61°C representing a decrease of 11.6°C from pure SA20H and T_{g2} with a mean value of –38.2 i.e., 8.1°C lower than the corresponding pure oligomer.

From the differences in the glass transitions between pure oligomers and corresponding oligomer/water system glass transitions it can be said that SA20C and SA20C-A2 have the same degree of plasticization and have more interaction with water than does SA20H.

Water phase characterization

Water transition temperatures of both pure water and oligomer/water systems are presented in Table 4. Only melting peak temperatures (T_{mp}) indicated a gel structure. From about 0.3 w/w oligomer (hard gels), T_{mp}s decrease with increasing oligomer concentration. This means that the increase of oligomer mass fraction of the system induces a topology that produces a capillary effect. The onset of crystallization temperature (T_{co}), which depend on water nucleation conditions, and the onset of melting temperature (T_{mo}) which depends on the degree of order of water crystals, will present a degree of variability related to the homogeneity of such topology.

Table 4 Transition temperatures of water in oligomer-water systems at different oligomer concentrations[a]

SA20C				SA20C-A2				SA20H			
Conc./ w/w	T_{co}/ °C	T_{mo}/ °C	T_{mp}/ °C	Conc./ w/w	T_{co}/ °C	T_{mo}/ °C	T_{mp}/ °C	Conc./ w/w	T_{co}/ °C	T_{mo}/ °C	T_{mp}/ °C
0.00	–21.7	–2.7	1.1	0.00	–21.7	–2.7	1.1	0.00	–21.7	–2.7	1.1
0.10[b]	–19.5	–12.0	0.3								
0.19	–14.7	–27.8	2.6								
0.21	–19.1	–30.1	2.7								
0.22	–18.1	–31.4	1.8	0.31	–16.1	–36.2	3.3	0.25	–18.1	–19.9	2.0
0.30	–21.2	–30.2	2.1								
0.40	–19.6	–30.9	1.0	0.30	–14.5	–25.0	2.7	0.39	–19.4	–23.4	0.5
0.50	–22.4	–25.6	–1.4								
0.59	–27.1	–30.7	–4.7	0.57	–19.5	–35.6	–2.7	0.58	–32.0	–28.2	–4.1
0.69	–43.2[c]	–18.1	–10.3								

[a] T_{co} is water crystallization onset; T_{mo} is water melting onset; T_{mp} is water melting peak
[b] Composition from liquid phase removed from 0.22 w/w SA20C-water sample
[c] Recrystallisation peak

For SA20C, up to 0.4 mass fraction, the changes in temperatures were not significant. The mean value for T_{co} was –18.7±0.9°C, for T_{mo} was –27.9±3°C and for T_{mp} was 1.7±0.4°C. The more significant change was observed for the sample with 0.69 w/w of SA20C in which the water crystallised on heating. These results point once more toward the effect of the gel topology indicating that the water molecules in the more concentrated gels was more confined, with a lower tendency to assume ordered structures.

The transition onsets and maximum peak of SA20C-A2 gels decreased with increase of oligomer content. By comparing these results with those recorded for SA20C/water system at equivalent compositions, one can verify that water has higher temperature transitions. The increase of transition temperature means that there is a higher order. This effect may be addressed to the hypothesis of a minimization of the contact surface between hydrophobic groups of the oligomer and water molecules.

As was observed for the other oligomer/water systems, SA20H showed an inverse relationship between temperature and system composition.

To estimate the amount of freezable and non-freezable water it was supposed that the heat of fusion, calculated for liquid water-ice transition, was identical for both pure and gel water. The content of freezable and non-freezable water and the average number of water molecules per oligomer molecule, was obtained from Eqs (1–3),

$$w_f = Q_w / \Delta H_w \quad (1)$$

$$w_{nf} = w_t - w_f \quad (2)$$

$$N_w/N_o=(w_{nf}/18)/(w_o/MW_o) \quad (3)$$

where w_f, w_{nf}, and w_t are mass of freezable, non-freezable and total water, respectively, and w_o is mass of oligomer; Q_w is the measured heat of transition in mJ; ΔH_w is the enthalpy of the ice-water transition ($\Delta H_{w\ cool}$=322 J g^{-1} and $\Delta H_{w\ heat}$=417 J g^{-1}, are mean values experimentally determined in this work); N_w and N_o are number of moles of water and oligomer respectively; and, MW_o is oligomer molecular mass.

Figure 4 shows the water enthalpy trends as a function of SA20C concentration from both cooling and heating scans. It can be noted that there is a good correlation among enthalpies until ca 0.5 w/w SA20C. Consequently, the water contents were calculated for concentrations between 0.5–0.69 w/w. Non-freezable water was directly related to the oligomer concentration as reported in Table 5. On the other hand, the number of moles water per mole of oligomer and the water freezable content are inversely proportional to the oligomer concentration.

The number of moles of water per mole of oligomer was slightly higher than that obtained for SA20C/water system for SA20C-A2 and slightly lower for SA20H.

Table 5 Water content in oligomer/water systems as a function of composition[a]

Olig. conc./ w/w	Cool			Heat		
	N_w/N_{SA20C}	Non-freeze/	Freeze/	N_w/N_{SA20C}	Non-freeze/	Freeze/
SA20C		%			%	
0.69	53.7	82.8	17.2	55.6	85.7	14.3
0.59	58.1	59.0	41.0	62.1	63.0	37.0
0.50	61.3	43.0	57.0	73.0	51.2	48.8
SA20C-A2						
0.57	62.0	50.0	50.0	68.0	55.2	44.8
SA20H						
0.58	56.0	56.5	43.5	64.0	64.5	35.5
0.39	60.0	28.0	72.0	88.0	40.9	59.1

[a]Freezable and non-freezable water is based on total water content in gel

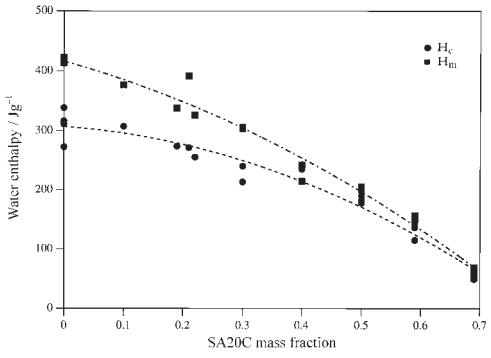

Fig. 4 Water enthalpy as a function of SA20C concentration on cooling and heating scans

Gel phase characterization

Figures 5–7 represent DSC traces recorded under cooling and heating modes for the three oligomer/water systems. A tail at the end of each process was more notable in the endothermic transitions. All figures illustrate the reversibility of the process which was observed in other thermo-reversible gels [13, 14].

Deng *et al.* [15, 16] found correlations between DSC onset temperatures and micellization processes, by a direct comparison of data collected from light scattering and DSC methods. For thermo-reversible gelation of polyoxyethylene/polyoxypropylene diblock copolymers they concluded that DSC peak represents a micellization process followed by the association of micelles which eventually resulted in a gel.

The thermodynamic properties as a function of oligomer/water composition are shown in Table 6. On cooling, the transition widths were more regular and narrow than on heating. At exception of T_{mgo} and ΔT_{mg}, there is a direct relationship between transition temperatures and SA20C concentration. The enthalpy on both cooling and heating are equivalent for 0.69 w/w SA20C concentration. For lower concentrations ΔH_{cg} began to be lower than ΔH_{mg}. The same was observed for SA20H/water system.

Table 6 Thermodynamic properties of the oligomer/water systems as a function of composition[a]

Olig. Conc/ w/w	T_{cgo}/°C	T_{cgp}/°C	ΔT_{cg}/°C	T_{mgo}/°C	T_{mgp}/°C	ΔT_{mg}/°C	ΔH_{cg}/ J g^{-1}	ΔH_{mg}/ J g^{-1}
SA20C								
0.69	27.8	16.4	29.9	7.8	24.0	35.5	29.3	29.3
0.59	21.4	13.3	20.9	8.4	17.6	25.7	26.5	27.8
0.50	19.2	10.4	19.9	10.0	15.2	21.4	25.3	26.8
0.40	14.7	7.4	19.3	7.1	15.0	24.3	17.2	20.1
0.30	13.0	6.3	19.9	5.2	13.9	28.7	16.2	20.7
SA20C-A2								
0.57	18.7	11.9	20.5	8.2	15.8	24.7	21.1	24.4
0.30	12.4	5.0	21.4	–7.0[b]	–2.8[b]	40.2[b]	14.0[b]	285.4[b]
0.31	11.2	2.0	21.5	–6.3[b]	–2.4[b]	46.9[b]	10.1[b]	331.0[b]
SA20H								
0.58	26.6	14.5	26.3	9.4	22.0	32.0	25.3	25.8
0.39	15.1	8.6	16.1	9.8	18.0	22.9	18.2	18.5
0.25	15.7	7.8	16.3	6.7	14.9	26.2	12.7	18.9

[a] T_{cgo}, T_{cgp}, are onset and peak temperature on cooling process, respectively; T_{mgo}, T_{mgp}, are onset and peak temperature on heating process, respectively; ΔT_{cg} and ΔT_{mg} are width transition temperature on cooling and heating, respectively; ΔH_{cg} and ΔH_{mg} enthalpies on cooling and heating, respectively
[b] Overlapped water and gel transitions

Samples at compositions lower than 0.3 w/w of SA20C presented an overlapping between water melting and gelation transition, even when crystallization of wa-

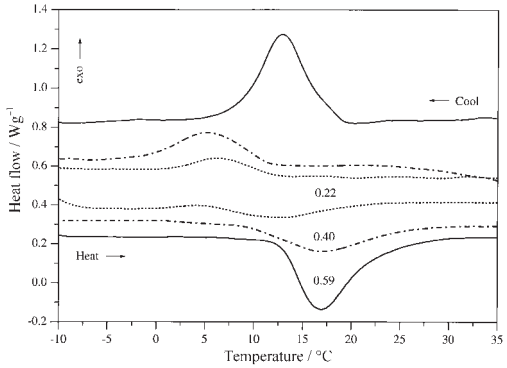

Fig. 5 DSC traces recorded under cooling (upper) and heating (lower) scans for SA20C/water system at various concentrations as indicated by the numbers on the traces

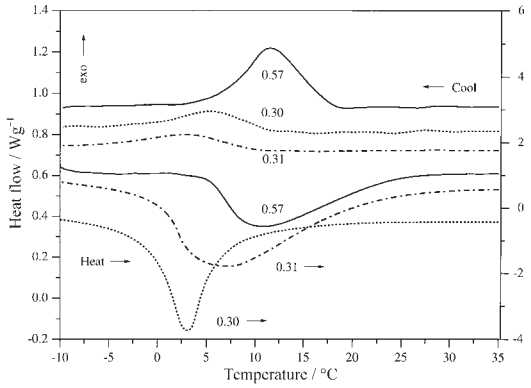

Fig. 6 DSC traces recorded under cooling (upper) and heating (lower) scans for SA20C-A2/water system at various concentrations as indicated by the numbers on the traces

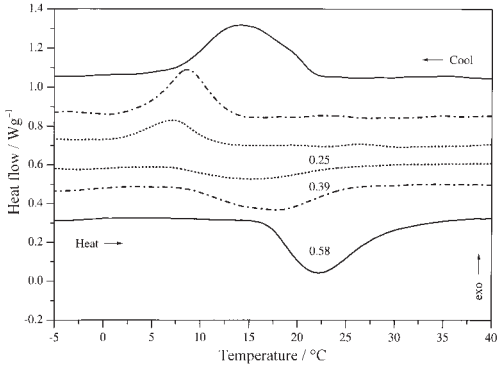

Fig. 7 DSC traces recorded under cooling (upper) and heating (lower) scans for SA20H/water system at various concentrations as indicated by the numbers on the traces

ter on cooling was not observed. At lower SA20C concentration, micelles are more disperse and it is possible that they function as nucleating agents for water crystallization. This process may compete with the association of micelles. When the concentration of oligomer increases, aggregation must prevail. This may explain the maximum on T_{mgo} and ΔT_{mg} and the initial slow change of base line observed on heating at higher concentrations, followed by a steep change (for example, trace for 0.59 w/w SA20C in Fig. 5).

Thermoreversible gelation of the SA20C-A2/water system are shown in Fig. 6. For concentrations at around 0.3 of oligomer mass fraction the endothermic transitions presented energies and peak temperatures equivalent to water melting (scale at right in Fig. 6 and Table 6). Consequently it was not possible to detect a gel transition. If the chemical nature of molecule associate with solution conditions would not permit an effective formation of bridging between micelles, free micelles could precipitate. At this point, the precipitate would favor nucleation of water crystals.

Basically, the thermo-reversible gelation profile of the SA20H/water system (Fig. 7) corresponds to the other systems. However, in this system at higher concentration a shoulder in the high temperature cooling process was observed. For higher oligomer concentration, the tail on endothermic peak at high temperature side assumed a more marked character. This observation may be correlated with energy transport within the gel.

Conclusions

A series of three amphiphilic oligomers consisting of two terminal non-ionic amphiphiles bridged with aliphatic or cycloaliphatic segments were investigated by TG and DSC analysis. Depending upon concentration and storage at room temperature, mixtures of water and of the oligomers tend to give rise to either soft or hard gels.

Glass transition temperatures were invariable in the concentration range of 0.2–0.6 oligomer mass fraction. Comparing the three symmetric block oligomer/water systems, it was shown that there was no significative difference between their T_gs: the mean value for T_{gh1} was –60.5±0.6°C and for T_{gh2} was –38.6±0.6°C. The equivalence in the behavior of the oligomers, suggest that it is related to their common end block, polyoxyethylene (20) stearyl ether. On the other hand, the central block characteristics (size, chemical nature, conformation) did not provide a contribution to the glass transition temperature of the gels in the concentration range studied, at least within the limits of the technique used.

The onset temperatures on cooling and heating and maximum melting temperature of water, decreased with increased oligomer concentration.

The number of moles of water per mole of oligomer was not dependent on the kind of the oligomer bridging central block. An inverse relationship of the water uptake with oligomer concentration was observed.

Given the normal error of thermodynamic calculations of water from DSC measurements, it can be concluded that between 60–70 moles of water interact directly with the oligomer chain, that is about 1.5 mole/mole of repeating oxyethylene unit.

The oligomers studied presented a thermo-reversible gelation with the possibility of precipitation at determined conditions.

DSC traces of gels indicated that the onset of one process overlapped the peak temperature of the other, principally at lower concentrations. This observation may be related to the mechanism of gel formation, considering the hypothesis that the DSC traces cover micellization followed by gelation.

References

1 B. J. Aungst, in: Michael Szycher (Ed.), High Performance Biomaterials – A Comprehensive Guide to Medical and Pharmaceutical Applications, Chap. 34, Technomic Publishing Company, Inc., Lancaster, USA 1991, p. 527.
2 L. H. Block, in: Alfonso R. Gennaro *et al.* (Ed.), Remington's Pharmaceutical Sciences, Chap. 88, 17th edition, Philadelphia College of Pharmacy and Science, 1985, p. 1567.
3 J. Crank and G. S. Park (Eds), Diffusion in Polymers, Academic Press, London 1968.
4 P. Ashton, J. Hadgraft and K. A. Walters, Pharm. Acta Helv., 61 (1986) 228.
5 M. Nguyen-Misra and W. L. Mattice, Macromolecules, 28 (1995) 1444.
6 E. A. Turi (Ed.), Thermal Characterization of Polymeric Materials, Vol. 1, 2nd ed. Academic Press, San Diego 1997.
7 B. Wunderlich and W. Chen, in A. I. Isayev, T. Kye, and S. Z. D. Cheng, eds., Recent Advances in Liquid Crystalline Polymers. ACS Symp. Series, Washington, DC 1996, p. 232.
8 J. D. Ferry, Viscoelastic Properties of Polymers, Wiley, New York 1980.
9 J. G. Nairn, in: Alfonso R. Gennaro *et al.* (Ed.), Remington's Pharmaceutical Sciences, Chap. 84, 17th edition, Philadelphia College of Pharmacy and Science, 1985, p. 1512.
10 T. Angell, J. Chem. Phys., 84 (1980) 268.
11 A. Keller, Faraday Discuss., 101 (1995) 1.
12 S. Callister, A. Keller and R. M. Hikmet, Makromol. Chem., Macromol. Symp., 39 (1990) 19.
13 S. Hvidt, E. B. Jørgensen, W. Brown and K. Schillén, J. Phys. Chem., 98 (1994) 12320.
14 J. M. Guenet, Macromol. Symp., 114 (1997) 97.
15 Y. Deng, G-E Yu, C. Price and C. Booth, J. Chem. Soc. Faraday Trans., 88 (1992) 1441.
16 Y. Deng, C. Price and C. Booth, Eur. Polym. J., 30 (1994) 103.